SF_6 Decomposition Gas Sensor Based on Metal-Organic Framework $Cu_3(TABTO)_2$Monolayer: A First-Principles Study

Degui Lin[1,2,#], Yumiao Zhang[1,2,#], Bensen Ye[1,2,#], Jiezhen Xia[1,2] and Qi Wu[1,2,*]

[1] *College of Science, Xizang University, Lhasa, 850000, China*

[2] *Tibet key Laboratory of Plateau Oxygen and Living Environment, College of Science, Xizang University, Lhasa 850000, China*

[*] Corresponding author email: wuqi@utibet.edu.cn.

[#]These authors contributed equally to this work.

Abstract

Detecting the decomposition gas of SF_6 insulating medium is essential for ensuring the safe and stable operation of the gas insulated switchgear (GIS).In this work, we utilized density functional theory (DFT) calculation based on first-principles theory to investigate the adsorption behavior and electronic properties of the five main sulfur hexafluoride (SF_6) decomposition components (H_2S, HF, SO_2, SOF_2 and SO_2F_2) on newly synthesized MX_2Y_2-type Metal-organic framework (MOFs), $Cu_3(TABTO)_2$. The stable adsorption structures were obtained by adsorption energy. The outcomes from charge transfer, density of states (DOS), and electron density difference (CCD) calculations provide a more comprehensive insight into the adsorption mechanism between the five decomposition gases and the $Cu_3(TABTO)_2$ monolayer. Meanwhile, we conclude that the chemical interaction of substrate with HF (-1.06 eV) and SO_2 (-0.83 eV). Furthermore, our results demonstrate that the substrate was highly sensitive to SO_2 because of the obvious change in electrical conductivity, and the selectivitystrength of $Cu_3(TABTO)_2$ to gases is HF > SO_2> H_2S > SO_2F_2> SOF_2. The recovery time of $Cu_3(TABTO)_2$ is 298 K (10.8 s) and 398 K (2.62 s) toward SO_2 and HF, respectively. The above calculation would be explored the chemical sensing application of $Cu_3(TABTO)_2$ monolayer in SF_6 decomposition gas sensing.

Keywords

Density functional theory (DFT), $Cu_3(TABTO)_2$ monolayer, SF_6 decomposition gases, gas-sensitive.

1. Introduction

Gas insulated switchgear (GIS) is commonly applied in highvoltage equipment and gas insulation systems. It relies heavily on the sulfur hexafluoride (SF_6) gas as the insulating mediumdue to their compound advantages, such as excellent insulation performance, strong electronegativity, arc extinguishing performance and non-toxicity [1,2]. However, the activecomponents of high-voltage GIS are usually made of copper and aluminum, while enclosures are manufactured from aluminum or steel[3,4]. Operating at elevated voltage levels, GIS is susceptible to internal arc faults, resulting in serious damage to the switches and theirimmediate surroundings, inevitablycausing the dissociation of SF_6 gas into low-fluoride sulfides (SF_n,n=1-5)[5, 6]. In addition, SF_n easily react with trace moisture and impurity present in GIS, ultimately forming sulfides (SO_2, SOF_2, SO_2F_2, H_2S) and HF[7, 8].Unfortunately, these decomposition gases will not only accelerate the aging of solid insulating materials, but also damage the quality of the surrounding air [9,10].Therefore, it is of great significance to

explore suitable gas-sensitive material for testing decomposition components of SF_6 to ensure the safe operation of GIS.

Currently, great efforts have been made to explore gas-sensitive materials for detecting SF_6 decomposition gases. For instance, Li et al.[11] investigated the adsorption characteristics of TiO_2 doped $HfSe_2$ monolayer for SF_6 decomposition gas. Their research comfirmed that the TiO_2-$HfSe_2$ material is capable of effectively adsorbing gases and possesses high sensitivity and stability. Moreover, Peng et al. [12] reported thatmetal Mg modified monolayer graphene significantly improved the electrical conductivity andenhanced the chemical stability of gas adsorption. In addition to graphene and two-dimensional dihalogens, metal oxide (such as zinc oxide [13] and titanium dioxide [5]) and metal-organic framework (MOFs) [14] have also been reported to capture SF_6 decomposition gases. Amongthese, MOFs have attracted broadlyattention based on their high porosity, structural diversity and tunable framework structure in recent years [15, 16]. Due to these advantages, MOFs have been applied in the fields of electrocatalysis [17, 18], gas adsorption [19] and chemical sensing [20].For example, using MOFs as a template, Pan et al. [21] synthesized A-Fe_2O_3 nanomaterials doped with different levels of rGO. This material has a strong electrical conductivity and electron transfer rate, showing superior responsiveness to NO_2. Zhai et al. [22] confirmed that MOFs (IO-66-NH_2) /PAN NM material has excellent selectivity and excellent response to SO_2 molecule.

Although many articles have reported that MOFs materials can be effectively used as gas-sensitive materials [23-25], there are few reports on MOFs as gas sensitive materials for SF_6 decomposition gases. Especially for MX_2Y_2-type MOF (M=metal, X, Y = N, O, S, and X ≠ Y) materials, it is still in the development stage [24,26]. Besides, the $Cu_3(TABTO)_2$ is an MX_2Y_2-type MOF and has been successfully prepared by Jiang et al. [27] in an inert gas environment. Interestingly, $Cu_3(TABTO)_2$ exhibits diverse properties such as high porosity, excellent electrical conductivity ($0.78 S/cm$) and charge carrier density ($5.0 \times 10^{17} \mathrm{cm}^{-3}$).In addition, the $Cu_3(TABTO)_2$ material has been successfully reported as a catalyst for carbon dioxide reduction [28].Based on this, $Cu_3(TABTO)_2$ exhibits catalytic, electrical and other properties. Adsorption of related gases by $Cu_3(TABTO)_2$ material leads to fluctuations in its electrochemical properties, resulting in detectable signals. Therefore, the feasibility of using $Cu_3(TABTO)_2$ as a gas sensitive material for detecting SF_6 decomposition gases was investigated.

In this study, the adsorption behavior and sensing properties of $Cu_3(TABTO)_2$ to five decomposition gases (SO_2, SOF_2, SO_2F_2, HF and H_2S) of SF_6 is predicated by density functional theory (DFT) calculation. The potential adsorption configurations of SO_2, SOF_2, SO_2F_2, HF and H_2S were examined based on the structure of $Cu_3(TABTO)_2$.The most stable adsorption configuration of SF_6 decomposed gases was determined by comparing the adsorption energy, and it was found that HF (-1.06 eV)and SO_2(-0.83 eV) exhibited ideal adsorption energy. Therefore, the density of states (DOS), charge density difference (CDD), charge transfer of HF@$Cu_3(TABTO)_2$ and SO_2@$Cu_3(TABTO)_2$systemswere systematically analyzed in order to understand the adsorption behavior of gas. Furthermore, the gas sensing properties of the substrate were assessed based on changes in work function, gas recovery time. It was concluded that $Cu_3(TABTO)_2$ material could serve as a suitable gas-sensitive material for detecting SO_2 at room temperature.

2. Computational details and methods

The spin-polarized density functional theory (DFT) calculations have been performed using the Vienna Ab-initio Simulation Package (VASP) code [29]. The Perdew-Burke-Ernzerhof (PBE) [30] functional form the generalized gradient approximation (GGA) [31], [32] was utilized for description the exchange correlation energy. The interaction of ionic core and valence

electrons were described by the projected augmented wave (PAW) [33] method. The van der Waals (vdW) effects between substrate and gas molecules was corrected using Grimme's DFT-D3 method [34], [35].The cutoff energy of the electronic wave function was truncated with a plane wave and was set500 eV, the convergence criterion of energy and force on each atom were 10^{-5} eV and 0.02eV $Å^{-1}$, respectively. The Brillouin zones were sampled using the3 × 3 × 1Monkhorst-Pack [36] meshes strategy, for the geometry optimization of all structures, while a 6 × 6 × 1k-point grid is used for the calculation of the density of states (DOS). A vacuum space of 20 Åwas set in the z-direction to prevent coupling between adjacent images. The Bader charge [37] [38] analysis was employed to evaluate the charge redistribution and quantify the amount of charge transfer between the gases and the substrate.

The adsorption energy (E_{ads}) of the SF_6 decomposition gas molecule attached to substrate was calculated by the following equation (1) [39]

$$E_{ads} = E_{Cu_3(TABTO)_2/gas} - E_{Cu_3(TABTO)_2} - E_{gas} \quad (1)$$

Where $E_{Cu_3(TABTO)_2/gas}$, $E_{Cu_3(TABTO)_2}$, and E_{gas} represent the total energies of the gas adsorption system, the $Cu_3(TABTO)_2$ monolayer, and the isolated gas molecules, respectively. The more negative the value of adsorption energy, the more stable the adsorption of gas molecules on the surface. Moreover, the charge density difference (CDD) was defined by this relation [40]

$$\Delta\rho = \rho_{Cu_3(TABTO)_2/gas} - \rho_{Cu_3(TABTO)_2} - \rho_{gas} \quad (2)$$

Where $\rho_{Cu_3(TABTO)_2/gas}$, $\rho_{Cu_3(TABTO)_2}$ and $\rho_{gas}$are the charge densityof substrate adsorbed gas, the isolated $Cu_3(TABTO)_2$, and the isolated gas molecules, respectively.

The work function (WF) φis determined in equation (3), measuring the Fermi level to the vacuum energy difference

$$\varphi = E_0 - E_F \quad (3)$$

$$\Delta\varphi = \frac{\varphi_a - \varphi_b}{\varphi_b} \%\# \quad (4)$$

Here, E_0 denote the vacuum energy level, and E_F means the Fermi level. The WF growth rate is calculated by formula (4), the $\varphi_a$and φ_b are the total work function of $Cu_3(TABTO)_2$ system after and before adsorbed gas molecule.

3. Results and discussion

3.1. The structure of gases and $Cu_3(TABTO)_2$

Fig. 1(a) illustrates the relaxed structure of the $Cu_3(TABTO)_2$ monolayer. The lattice parameters (a = b) of the $Cu_3(TABTO)_2$ monolayer with a unit cell were measured as 13.45Å. These structural parameters are in excellent agreement with the previously reported literature [27]. The substrate possesses a considerable number of pore structures, maintaining outstanding gas permeability and ensuring that a greater amount of gas can be

adsorbed within a short period. Additionally, the electron localization function (ELF) of $Cu_2(TABTO)_2$ was also calculated, as show in Fig. 1(c).The O atom has a stronger charge localization in its vicinity compared to the N atom, and the Cu atom has almost no charge localization around it. Therefore, we select two kinds of possible adsorption sites on the surface of the $Cu_3(TABTO)_2$, which are: (i) the site C1 is directly above the O atom, (ii) the site C2 above the center of Cu atom as the adsorption site of SF_6 decomposition gases as presented in Fig. 1(a). Fig.1(d) depicts the band structure and total density of states (TDOS) of the $Cu_3(TABTO)_2$ monolayer, the conduction band minimum (CBM) and the valence band maximum (VBM) were located at the r point of the Brillouin zone. A direct band gap of 0.485 eV, indicating the substrate exhibits obvious semiconducting property and conducive to electron transfer between valence band and conduction band. The peak of TDOS near Fermi level confirms the position of CBM and VBM, and the asymmetry of spin up and spin down peaks suggests that $Cu_3(TABTO)_2$has certain magnetic properties.

The SF_6 decomposition gas structure illustrates in Fig. 1(b). The H_2S and SO_2 molecules exhibit a V-shaped structure, with the bond angle for H-S-H and O-S-O are 91.642° and 119.25°, respectively, the S-H bond and S-O bond length of 1.34 Å and 1.45 Å, respectively. The SOF_2 molecule possesses a pyramid configuration and the SO_2F_2 molecule possesses a planar triangular spatial configuration, their bond lengths and bond angle as summarize in Fig. 1(b). HF gas has a basic plane structure, its H-F bond length of 0.94 Å. The gas structure described above is consistent with the literature.

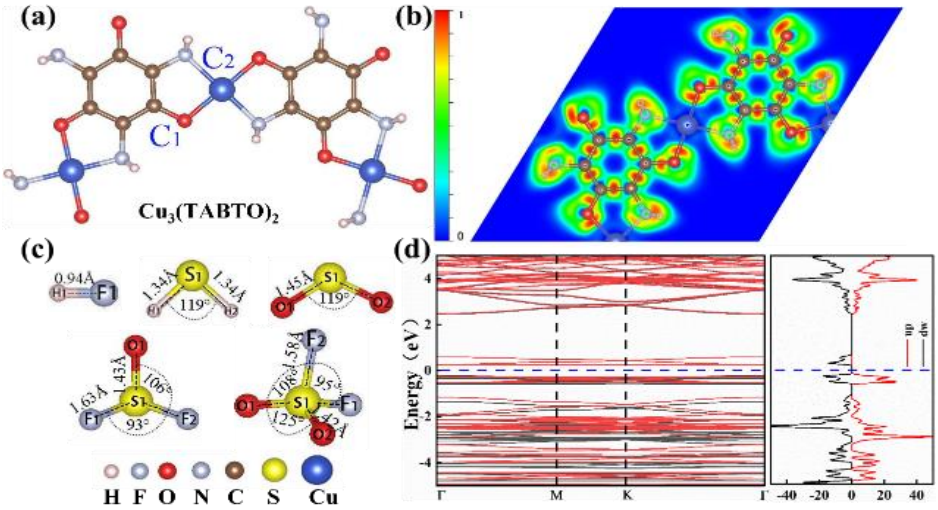

Figure 1. (a) The optimized structure of $Cu_3(TABTO)_2$. (b) The optimized structure of HF, H_2S, SO_2, SOF_2, SO_2F_2 molecules. (c) Electron localization functions (ELFs) for $Cu_3(TABTO)_2$. (d) The diagram of band structure for $Cu_3(TABTO)_2$ near fermi level and total density of states in corresponding range. The fermi level is set to zero.

3.2. Gases adsorption Performance on the $Cu_3(TABTO)2$monolayer

After studying the configuration of the $Cu_3(TABTO)_2$ monolayer and the gas molecules, the adsorption behavior of five gases on $Cu_3(TABTO)_2$were investigated. Taking into account the aforementioned regarding adsorption sites, two distinct adsorption models were devised for H_2S, HF and SO_2 gases: one in which the S atom and F atom pointed downward the substrate and another in which the gas is oriented parallel to the surface. In the case of SOF_2 and SO_2F_2, the two possible directions are to keep the S and O atoms towards the adsorption site. The possible adsorption mode for each gas is shown on Fig.2.

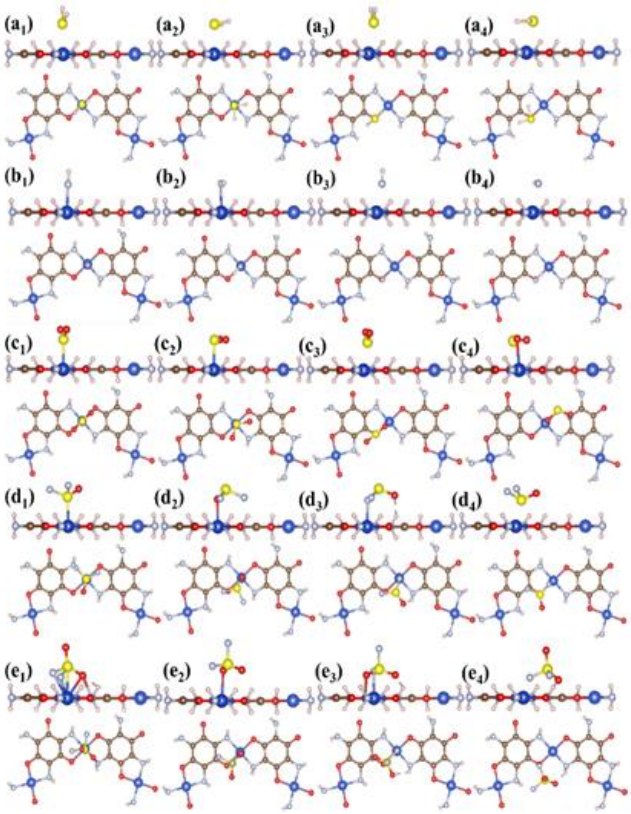

Figure 2. Different configurations of $Cu_3(TABTO)_2$ adsorbed gas for (a) H_2S; (b) HF; (c) SO_2; (d) SOF_2; (e) SO_2F_2.

After structural relaxation, the most stable adsorption configuration of each gas was obtained by comparing the adsorption energy, as shown in Fig. 3.The most preferred adsorption configuration for HF, SOF_2 and SO_2F_2molecules were stably adsorb at the O location, while for $SO_2$and H_2S the most favorable was O site and H atom. Since the H_2S and HF molecules are attached to the substrate via the H atom, they do not form bonds with the atoms of $Cu_3(TABTO)_2$. Fig. 3demonstrates the average adsorption distances of H_2S, HF, SO_2, SOF_2, and SO_2F_2 to $Cu_3(TABTO)_2$ are 2.377Å, 0.374Å, 2.206Å, 2.76Å, and 2.665Å, respectively. Meanwhile, the calculated variations in bond lengths prior to and subsequent to the adsorption of gas molecules have been shown in Fig. 3. The adsorption height of the SF_6 decomposition gases and the changes in bond lengths before and after adsorption indicate that HF and SO_2 molecules have chemical interactions with the surface. Furthermore, the calculation stable adsorption energy for HF, H_2S, SO_2, SOF_2 and SO_2F_2were -1.06, -0.34, -0.83, -0.25 and -0.34eV, respectively. Except for $Cu_3(TABTO)_2$@$SO_2$and $Cu_3(TABTO)_2$@HF, the low adsorption energies in the remaining three examples indicated the role of long-range interaction between the gases and the $Cu_3(TABTO)_2$ monolayer.

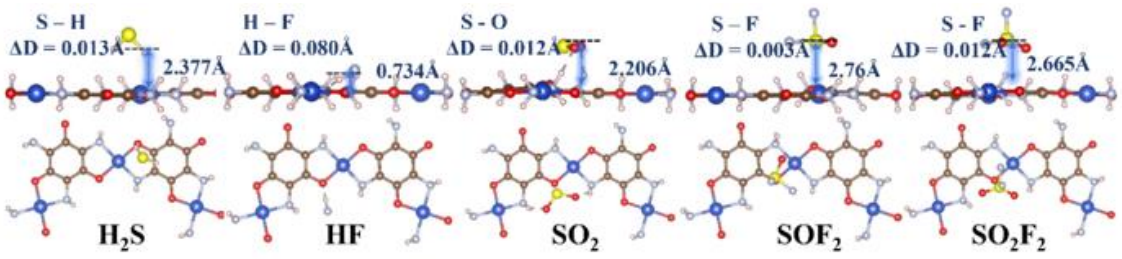

Figure 3. The most stable adsorption configurations of SF_6 decomposition gas on $Cu_3(TABTO)_2$.

In order to elucidate the adsorption mechanism of gases, the Bader charges are calculated, and the results are summarized in Fig. 4 (a). For all gas molecules, electrons are transferred from the $Cu_3(TABTO)_2$ to the HF, H_2S, SO_2, SOF_2 and SO_2F_2 molecules, with values of 0.092 e, 0.022 e, 0.200 e, 0.068 e, 0.012 e, respectively. The evident chemisorption behavior in these cases was supported by the substantial charge transfers, particularly in the systems of $SO_2$and HF adsorbed on $Cu_3(TABTO)_2$ monolayer. Furthermore, Fig. 4 (b) illustrates the Bader charges before at the Cu and O site of the substrate material and prior to gas adsorption. It is observed that the Cu atom within the system maintains stable state with 10 electrons, while the O atom exists in an unsaturated state characterized by 7 electron spin polarization, thereby facilitating enhanced gas molecules adsorption at the C2 site. Additionally, it can be noted that in HF gas, the H atom donates electrons to the F atom, resulting in its 1s orbital approaching an empty orbital configuration, indicative of strong electron philicity. Consequently, in $HF@Cu_3(TABTO)_2$, the H atom preferentially interacts with an O atom on the substrate. For SO_2 gas, S atom donates electrons to O atoms leading to increased availability of empty orbitals on S atoms, thus during SO_2 adsorption, S atoms exhibit a tendency to interact with the O atoms present in the system.

To intuitively demonstrate the change of charge transfer after gas adsorption, we investigated the Charge density difference (CDD)and the variation in charge amount for each atom (ΔQ),as depicted in Fig. 4(a) and (c).For SO_2 adsorbed on the $Cu_3(TABTO)_2$,the yellow area of charge accumulation appears around SO_2 molecule, while an obvious charge depletion region can be observed on $Cu_3(TABTO)_2$, consistent with the result shown in Fig. 4(c). Furthermore, the increase in charge of the O atom within the SO_2 molecule can be attributed to electron transfer from S atoms that acquire charges from the surface before transferring them to O atoms.For HF adsorption, yellow regions surrounding the gas molecules, indicating that the substrate has a relatively obvious charge transfer to the HF gas; the ΔQ analysis reveals that it is predominantly H atoms that gain electrons in the substrate. In contrast, for H_2S gas, minimal charge interaction is detected;however, for SO_2F_2 and SOF_2 gases, CDD primarily concentrated around these gas molecules--a finding corroborated by ΔQ analysis.The characteristics of CDD suggest that the adsorption capacities of SO_2 and HF is derived from the S-O bond and the interaction between H and O, respectively. Meanwhile, combined with the adsorption energy of the gas adsorption system and Bader charge transfer, it is indicated that there is a weak physical interaction between H_2S, SO_2F_2 and SOF_2 molecules and the surface.

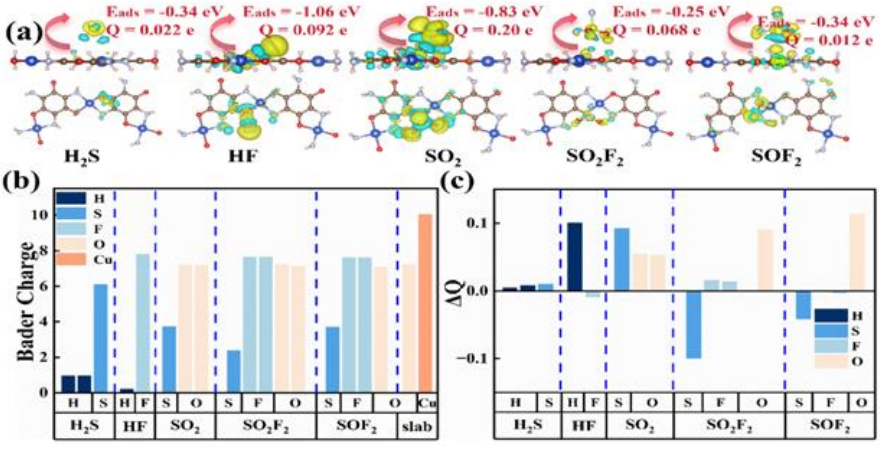

Figure 4. (a) Charge density difference (CDD) of various adsorption systems, and the isosurface value is 0.003 e Å $^{-3}$, where blue and yellow areas represent the loss and reception of electrons, respectively; (b) The Bader charge associated with each atom in the gas molecule, as well as that of the O and Cu atoms within the substrate. (c) Charge transfer of atoms on the adsorbed gases.

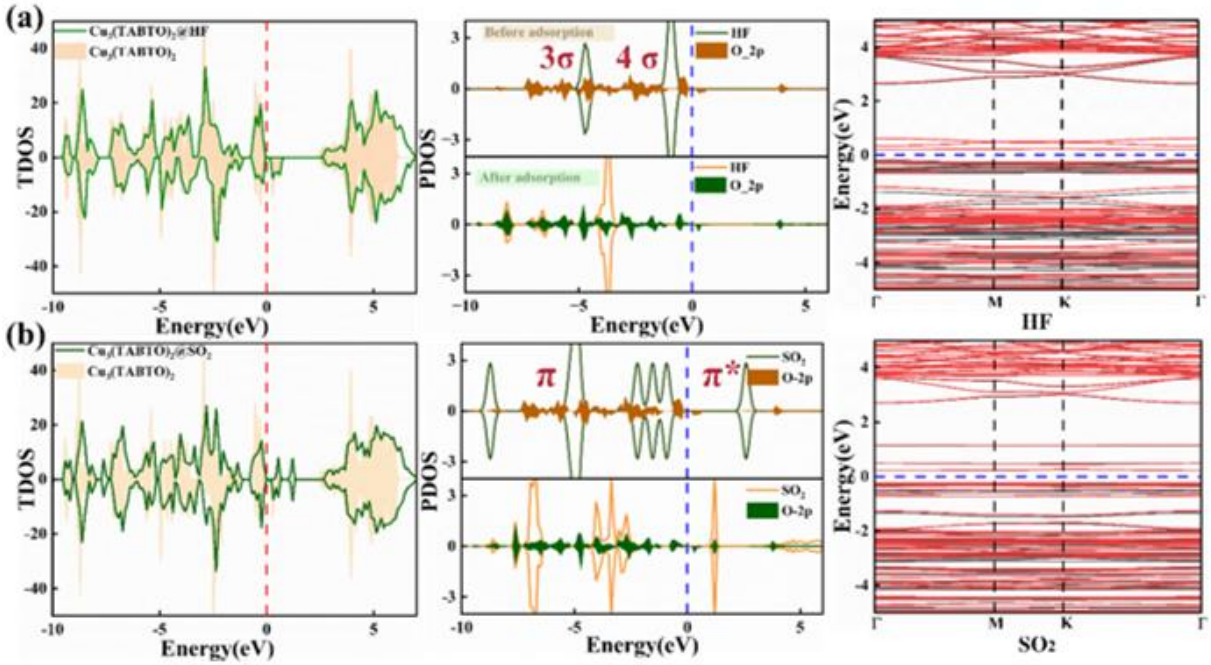

Figure 5. The TDOS, PDOS and band structure of adsorption systems (a) HF, (b) SO_2. The Fermi level was set to zero.

To gain a more profound understanding of the interaction between the adsorbed gas molecule and the $Cu_3(TABTO)_2$ monolayer, we analyzed the density of states and band structure. Fig. 5(a - e) displayed the spin-polarized total densities of states (TDOS), projected density of states(PDOS) and band structure for various adsorption systems. Specifically, Fig.5(a) illustrates the DOS for HF@$Cu_3(TABTO)_2$, it can be seen that prior to HF adsorption, the 2p orbitals of oxygen atom at the substrate adsorption site are continuously occupied between -7 and 0eV, while isolated molecular orbitals of 3σ and 4σ of HF occupy within energy level -5 to 0eV. Following HF adsorption, the orbital characteristics of HF@$Cu_3(TABTO)_2$ become delocalized in relation to the isolated surface orbitals. Furthermore, it is observed that the molecular orbitals are hybridized with the 2p orbitals of O, this results in a splitting of the original 3σ orbital into two new distinct orbitals as well as the molecular orbitals downward shift to lower energy position. Additionally, the π and non-bonding type orbitals of the SO_2 molecular, which occupy energy levels between -5 and 0eV, are summarized in Fig. 5 (b). After the adsorption of SO_2, the TDOS reveals new peaks in the orbitals structure of the adsorption system at -7.5 and 1.6 eV, respectively. The PDOS analysis indicates that at -7.5 eV, the πtype orbitals of the SO_2 molecule hybridizes with the 2p orbitals of the substrate, resulting in a downward shift and subsequent splitting into a new orbital configuration. Furthermore, the new peak observed at 1.6 eV arises from interactions between π* type and O_2p orbitals, leading to a downward movement to this energy level. The changes in the molecular orbitals of SO_2 and HF both proved that the gas molecules gain electrons during the adsorption process. In summary, the TDOS and PDOS analyses of HF@$Cu_3(TABTO)_2$ and SO_2@$Cu_3(TABTO)_2$ show that the interaction between HF and SO_2 molecules and the substrate from the mutual hybridization of molecular orbitals with O_2p orbitals on $Cu_3(TABTO)_2$. However, for the remaining three gas adsorption systems, their TDOS is shown in Fig.6(a - c). When the gas is adsorbed, the TDOS of the adsorption system changes slightly, but it remains stable compared with the original peak, indicating that the interaction between H_2S, SO_2F_2 and SO_2F molecules and the surface belongs to Van der Waals.

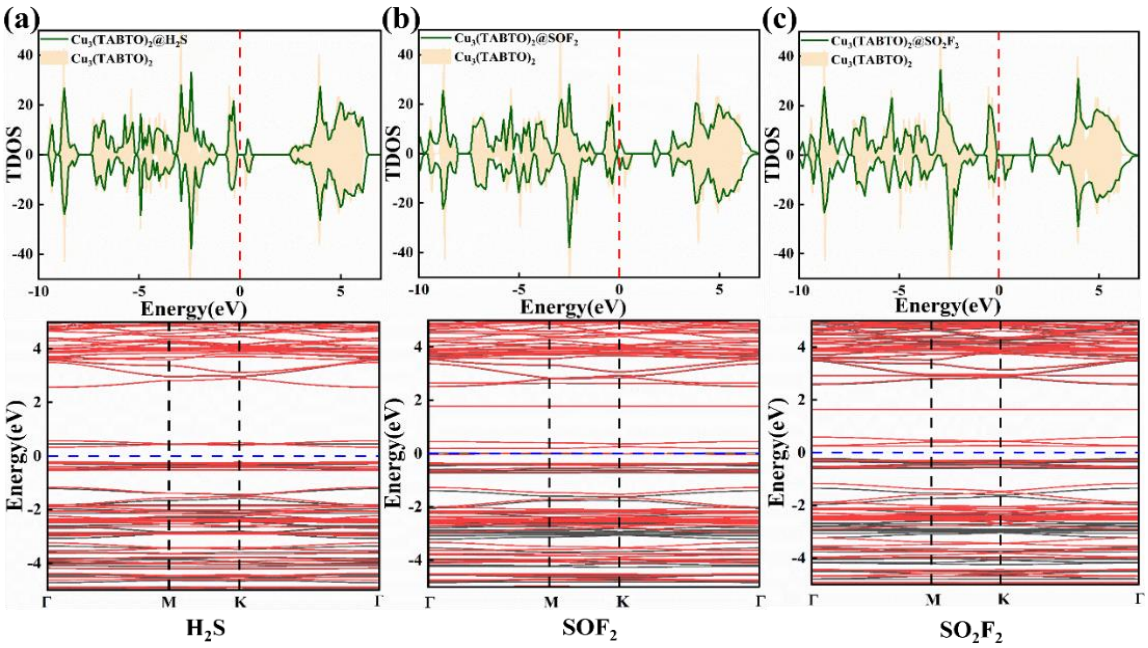

Figure 6. The TDOS and band structure of adsorption systems (a) H_2S, (b) SOF_2, (c) SO_2F_2. The Fermi level was set to zero.

3.3. Gas-Sensing Prediction of $Cu_3(TABTO)_2$ to SF_6 Decomposition Products

For resistive gas sensors, measuring the change of electrical conductivity after adsorbing gas is one of the ways to evaluate their response characteristic, hence, the work function (WF) was calculated to measure the adsorption sensitivity of SF_6decomposition gases. It is known that the WF represents the least energy required for a substance to eject an electron from its interior and into vacuum and also the ability of the material to bind electrons. In order to clearly demonstrate the ability of $Cu_3(TABTO)_2$ monolayer to detect gases, the WF of the adsorption system and its growth rate are summarized in Fig. 7(a).

The WF of the $Cu_3(TABTO)_2$ monolayer was measured to be 3.917 eV. After adsorbed HF, H_2S, SO_2, SOF_2 and SO_2F_2 on the $Cu_3(TABTO)_2$ monolayer, the WF increased to 4.323, 4.210, 4.414, 4.344 and 3.928 eV, respectively. It is noted that the surface adsorption gas, the WF of the SO_2@$Cu_3(TABTO)_2$ system is the largest and the WF of the SO_2F_2@$Cu_3(TABTO)_2$ system is the smallest. Furthermore, the greater the change in work function, the more pronounced the alteration in conductivity. It is evident that the exceptional respond performance of $Cu_3(TABTO)_2$ monolayer towards the SO_2, HF and SOF_2molecules could be validated by the larger growth rates$\Delta\varphi$of 12.69%, 10.37% and 10.9%. Meanwhile, within gas adsorption systems, the band structure of SO_2 (0.464 eV), HF (0.406 eV) and SOF_2 (0 eV) molecules has decreased compared to the original surface, indicating an enhancement in electrical conductivity and adsorption capacity of these systems. The WF growth rate and bandgap for H_2S were 7.48% and 0.547 eV; for SO_2F_2, there were 0.28% and 0.473 eV, suggesting that after H_2S adsorbed, there is an increase in bandgap leading to less stable adsorption while showing negligible response to SO_2F_2 molecule adsorption. Additionally, weak physical adsorption was observed for SOF_2 on the substrate material, hence $Cu_3(TABTO)_2$ monolayer only has the potential to be developed as a WF-based gas sensor for detection SO_2 and HF.

In addition to exhibiting excellent sensitivity, a high-performance gas sensor also requires fast desorption capability. Hence, the recovery time was calculated as defined in Equation (5):

$$\tau = A^{-1} \exp\left(\frac{|E_{ads}|}{k_B T}\right) \quad (5)$$

Where, the A^{-1}(10^{12} s^{-1})represent the apparent frequency, the E_{ads} is adsorption energy of gases. It can be deduced from the formula that the recovery time can be minimized by elevating the temperature when other parameters remain constant. As depicted inFig.7(b), it can be discerned that the SO_2,HF, H_2S, SOF_2 and SO_2F_2exhibittherecovery time of 10.8 s,8.34×10^4s,5.6×10^{-8}s,5.6×10^{-8}s and 1.69×10^{-8}sat room temperature, respectively. It is obvious that SO_2 has excellent recovery time at 298 K. Moreover, as the temperature elevates, the recovery time of all gases progressively decreases. It's noteworthy that at 398 K, the recovery time for HF is reduced to a mere 2.62 seconds. This implies that the $Cu_3(TABTO)_2$ monolayer can be reused as a gas sensing material for SO_2 detection at 298 K and for HF detection at 398 K. On the other hand, the H_2S, SOF_2 and SO_2F_2exhibitbrevity recovery times at room temperatures, further suggesting that $Cu_3(TABTO)_2$ cannot detect these three gases.

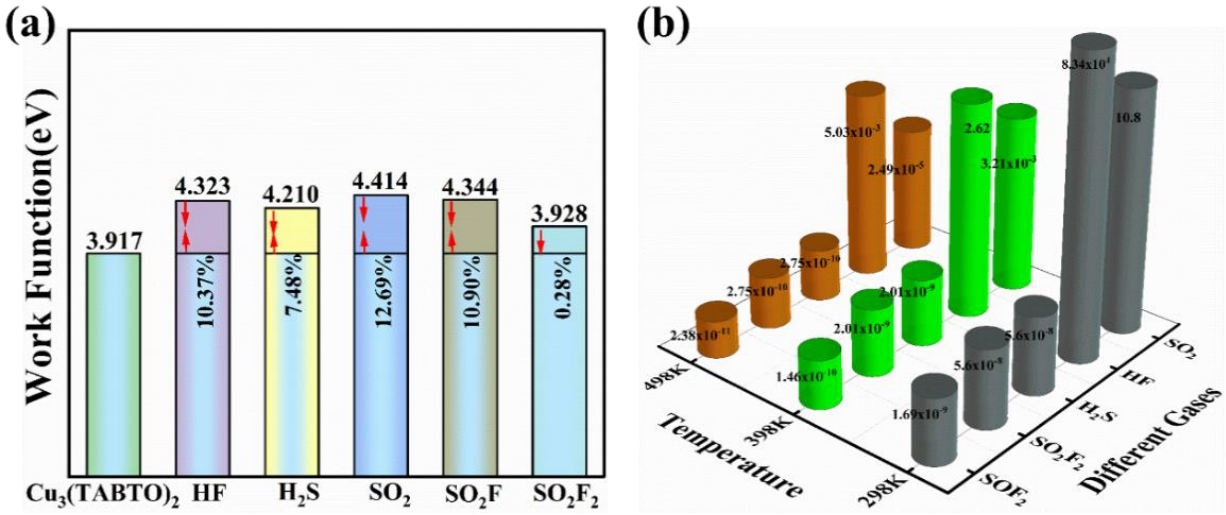

Figure 7. (a) Work function and WF growth rate of adsorption systems;
(b) The predicted recovery time of various optimized systems.

4. Conclusions

In this paper, the interaction mechanism between SF6 decomposition gases molecule and Cu3(TABTO)2 monolayer surface was invested based on DFT calculation. The optimal adsorption configuration of Cu3(TABTO)2for these five gases is discussed, and the best adsorption system was determined based on comparison of adsorption energy. The calculation results of electron transfer, charge density difference and density of states were analyzed to further explore the electronic characteristics of the adsorption systems. Furthermore, the sensing mechanism of Cu3(TABTO)2 monolayer for five gases was examined.

The conclusion obtained provides a theoretical basis for the potential application of Cu3(TABTO)2 as the detection sensor for SF6 decomposition gas. The following are the main conclusions:

(1) Based on the analysis of adsorption energy and charge transfer, it is inferred that the adsorption of Cu3(TABTO)2 monolayer for H2S, SO2F and SO2F2belong to physical adsorption, while for HF and SO2can be categorized as chemical adsorption. Moreover, the

TDOS and PDOS analyses validate that the 2p orbital of the O atom on the surface exhibits significant hybridization with the HF and SO2 molecular orbitals, implying the strong chemical interaction between substrate and HF, SO2.

(2) The WF analysis offers the sensing mechanism of Cu3(TABTO)2 monolayer

as resistance-type chemical sensor. Furthermore, Cu3(TABTO)2has excellent response to SO2and HF molecules.

(3) The Cu3(TABTO)2 can be promising gas sensing material to HF at 389 K and

SO2at 298 K, as evidenced by the recovery time for SO2 and HF.

In summary, this study holds considerable promise for the advancement of SF6 decomposition gas sensors, introducing novel insights and strategies for the design and development of Cu3(TABTO)2 materials.

References

[1] C. Y. Chuah, Y. Lee and T.-H. Bae, Chemical Engineering Journal, 2021, 404, 126577.

[2] S. Kim and P. Nagorny, Organic Letters, 2022, 24, 2294-2298.

[3] M. Maiss, L. P. Steele, R. J. Francey, P. J. Fraser, R. L. Langenfelds, N. B. A. Trivett and I. Levin, Atmospheric Environment, 1996, 30, 1621-1629.

[4] D. Beslija, D. Gorenc, M. Muratovic and M. Kapetanovic, IEEE Transactions on Power Delivery, 2020, 35, 1619-1624.

[5] W. Cao, Y. Gui, T. Chen, L. Xu and Z. Ding, Applied Surface Science, 2020, 524, 146570.

[6] Y. Wang, Y. Gui, C. Ji, C. Tang, Q. Zhou, J. Li and X. Zhang, Applied Surface Science, 2018, 459, 242-248.

[7] J. Tang, F. Zeng, X. Zhang, J. Pan, Q. Yao, X. Hou and Y. Tang, IEEE Transactions on Dielectrics and Electrical Insulation, 2014, 21, 1226-1234.

[8] C. Beyer, H. Jenett and D. Klockow, IEEE Transactions on Dielectrics and Electrical Insulation, 2000, 7, 234-240.

[9] Z. Cui, X. Zhang, Z. Cheng, Y. Li and H. Xiao, Spectrochimica Acta Part A: Molecular and Biomolecular Spectroscopy, 2019, 215, 187-195.

[10] S. Xiao, X. Zhang, J. Tang and S. Liu, Energy Reports, 2018, 4, 486-496.

[11] W. Li, H. Qiao, X. Zhang, P. Wang and L. Q. Tao, IEEE Sens. J. (USA), 2024, 24, 15811-15818.

[12] X. Peng, D. Liu, F. Zhao and C. Tang, International Journal of Quantum Chemistry, 2022, 122.

[13] D. Chen, X. Zhang, J. Tang, H. Cui, S. Pi and Z. Cui, ACS Omega, 2018, 3, 18739-18752.

[14] S. Grubisic, R. Dahmani, I. Đorđević, M. Sentic and M. Hochlaf, Physical Chemistry Chemical Physics, 2023, 25.

[15] H. Li, M. Eddaoudi, M. O'Keeffe and O. M. Yaghi, Nature, 1999, 402.

[16] O. Yaghi, M. O'Keeffe, N. Ockwig, H. Chae, M. Eddaoudi and J. Kim, Nature, 2003, 423, 705-714.

[17] Y. Tian, C. Zhu, L. Yan, J. Zhao and Z. Su, Journal of Materials Chemistry A, 2019.

[18] G. Gao, E. R. Waclawik and A. Du, Journal of Catalysis, 2017, 352, 579-585.

[19] X. Zhang, R. B. Lin, J. Wang, B. Wang, B. Liang, T. Yildirim, J. Zhang, W. Zhou and B. Chen, Advanced Materials, 2020, 32.

[20] P. Kumar, A. Deep and K.-H. Kim, TrAC Trends in Analytical Chemistry, 2015, 73, 39-53.

[21] Z. Pan, D. Wang, D. Zhang, Y. Yang, H. Yu, T. Wang and X. Dong, Sensors and Actuators B: Chemical, 2024, 405, 135378.

[22] Z. Zhai, J. Wang, Y. Sun, X. Hao, B. Niu, H. Xie and C. Li, Applied Surface Science, 2023, 613, 155772.

[23] X. Peng, X. Wu, F. Yang, Y. Tian, M. Zhang and H. Yuan, Chinese Journal of Structural Chemistry, 2024, 43, 100251.

[24] B. Yan, Accounts of chemChemical Research17, 50 11, 2789-2798.

[25] I. Stassen, N. C. Burtch, A A. Talin, P. Falcaro, M. D. Allendorf and R. Ameloot, Chemical Society reviews, 2017, 46 11, 3185-3241.
[26] X. Sun, K.-H. Wu, R. Sakamoto, T. Kusamoto, H. Maeda, X. Ni, W. Jiang, F. Liu, S. Sasaki, H. Masunaga and H. Nishihara, Chemical Science, 2017, 8, 8078-8085.
[27] Y. Jiang, I. Oh, S. H. Joo, Y.-S. Seo, S. H. Lee, W. K. Seong, Y. J. Kim, J. Hwang, S. K. Kwak, J. W. Yoo and R. S. Ruoff, Journal of the American Chemical Society, 2020.
[28] G. Jinghan, L. Cheng, K. Li, Y. Wang and Z. Wu, Journal of The Electrochemical Society, 2022.
[29] J. Hafner, Journal of computational chemistry, 2008, 29, 2044-2078.
[30] B. Hammer, L. B. Hansen and J. K. Nørskov, Physical Review B, 1999, 59, 7413-7421.
[31] Juan, Kaxiras and Gordon, Physical review. B, Condensed matter, 1995, 51 15, 9521-9525.
[32] J. P. Perdew, K. Burke and M. Ernzerhof, Physical Review Letters, 1997, 78, 1396-1396.
[33] G. F. J. Kresse, Physical Review, B. Condensed Matter, 1996, 54.
[34] S. Ehrlich, J. Chem. Phys., 2010, 132, 1.
[35] S. Grimme, S. Ehrlich and L. Goerigk, Journal of computational chemistry, 2011, 32, 1456-1465.
[36] J. Chadi, Phys. Rev. B, 1977, 16.
[37] R. Jayan and M. M. Islam, The Journal of Physical Chemistry C, 2021, 125.
[38] W. Xu, T. Feng, J. Xia, R. Cao and Q. Wu, Physical chemistry chemical physics : PCCP, 2024, 26.
[39] W. Li, H. Qiao, X. Zhang, P. Wang and L. Q. Tao, IEEE Sens. J. (USA), 2024, 24, 15811-15818.
[40] S. Thomas, F. Mayr and A. Gagliardi, SOLID STATE COMMUNICATIONS, 2023, 363.